LA-UR- 08-4853

Approved for public release;
distribution is unlimited.

Title:	Surface Complexation of Neptunium (V) onto Whole Cell Components of Shewanella Alga
Author(s):	Donald T. Reed Randhir P. Deo (Arizona State University) Warinthorn Songkasiri (Unaffiliated) Bruce E. Rittmann (Arizona State University)
Intended for:	Publication as a journal article in Geochimica Cosmochimica Acta

Los Alamos
NATIONAL LABORATORY
EST. 1943

Form 836 (7/06)

Surface Complexation of neptunium (V) onto whole cells and cell components of *Shewanella alga*

Randhir P. Deo[a], Warinthorn Songkasiri[b], Bruce E. Rittmann[a*], and Donald T. Reed[c]

[a] Center for Environmental Biotechnology, Biodesign Institute, Arizona State University, Tempe, AZ 85287-5701 U.S.A.

[b] National Center for Genetic Engineering and Biotechnology, Biochemical Engineering and Plant Research and Development Unit, King Mongkut's University of Technology Thonburi, Bangkok, 10150 Thailand

[c] Los Alamos National Laboratory, Environmental and Earth Sciences Division, Carlsbad Environmental Monitoring and Research Center, Carlsbad, NM 88220 U.S.A.

* Corresponding author

Abstract

We systematically quantified surface complexation of neptunium(V) onto whole cells of *Shewanella alga* strain BrY and onto cell wall and extracellular polymeric substances (EPS) of *S. alga*. We first performed acid and base titrations and used the mathematical model FITEQL with constant-capacitance surface-complexation to determine the concentrations and deprotonation constants of specific surface functional groups. Deprotonation constants most likely corresponded to a carboxyl site associated with amino acids (pK_a ~ 2.4), a carboxyl group not associated with amino acids (pK_a ~ 5), a phosphoryl site (pK_a ~ 7.2), and an amine site (pK_a > 10). We then carried out batch sorption experiments with Np(V) and each of the *S. alga* components at different pHs'. Results show that solution pH influenced the speciation of Np(V) and each of the surface functional groups. We used the speciation sub-model of the biogeochemical model CCBATCH to compute the stability constants for Np(V) complexation to each surface functional group. The stability constants were similar for each functional group on *S. alga* bacterial whole cells, cell walls, and EPS, and they explain the complicated sorption patterns when they are combined with the aqueous-phase speciation of Np(V). For pH < 8, NpO_2^+ was the dominant form of Np(V), and its log K values for the low-pK_a carboxyl, other carboxyl, and phosphoryl groups were 1.75, 1.75, and 2.5 to 3.1, respectively. For pH greater than 8, the key surface ligand was amine $>XNH_3^+$, which complexed with $NpO_2(CO_3)_3^{5-}$. The log K for $NpO_2(CO_3)_3^{5-}$ complexed onto the amine groups was 3.1 to 3.6. All of the log K values are similar to those of Np(V) complexes with aqueous carboxyl and N-containing carboxyl ligands. These results point towards the important role of surface complexation in defining key actinide-microbiological interactions in the subsurface.

1. INTRODUCTION

The presence of actinides as subsurface contaminants has become a major environmental concern due to their long radioactive half-lives, energetic emissions, and chemical toxicity (Murray, 1989). The general objective in remediation of radioactive elements is recovery, immobilization, or isolation of the actinides from environmental receptors, including humans (Collins, 1960; Banaszak et al., 1999; Pearl, 2000).

This research reported here contributes to understanding actinide-microorganism interactions that may affect immobilization of actinides: surface complexation of neptunium (Np), an actinide, onto bacterial surfaces. We quantified Np(V) complexation to the surface components of *Shewanella alga* strain BrY: bacterial whole cells, purified cell walls, and isolated extracellular polymeric substances (EPS). In particular, we characterized surface acid/base groups active in complexing Np(V) according to their concentration, acid/base deprotonation constant (pK_a), and complexation stability constant (log K) for relevant Np(V) species.

Bacterial surfaces consist of heterogeneous mixtures of proton-active surface sites, potentially including carboxyl, phosphoryl, hydroxyl, and amino, groups (*5-7*). Their deprotonation reactions are

$$\equiv X - COOH^0 \rightarrow \equiv X - COO^- + H^+ \quad (1)$$

$$\equiv X - PO_4H^0 \rightarrow \equiv X - PO_4^- + H^+ \quad (2)$$

$$\equiv X - OH^0 \rightarrow \equiv X - O^- + H^+ \quad (3)$$

$$\equiv X - NH_3^+ \rightarrow \equiv X - NH_2 + H^+ \quad (4)$$

where $\equiv X$ represents the bacterial surface. The deprotonation or acid-dissociation constants for the reactions are, respectively,

$$K_1 = \frac{[\equiv X - COO^-]\{H^+\}}{[\equiv X - COOH^0]} \quad \textbf{(5)}$$

$$K_2 = \frac{[\equiv X - PO_4^-]\{H^+\}}{[\equiv X - PO_4H^0]} \quad \textbf{(6)}$$

$$K_3 = \frac{[\equiv X - O^-]\{H^+\}}{[\equiv X - OH^0]} \quad \textbf{(7)}$$

and $$K_4 = \frac{[\equiv X - NH_2]\{H^+\}}{[\equiv X - NH_3^+]} \quad \textbf{(8)}$$

where the square brackets represent the concentration of surface species in moles per liter of solution and the non-square brackets represent the activity of the aqueous species. Concentrations are used for surface species, because activity coefficients are difficult to define for surface species.

Daughney et al. (1998) used the computer program FITEQL version 4.0 (Herbin and Westall, 1994) to find the deprotonation constant and concentration for each surface site on cell surfaces of *Bacillus licheniformis*, a Gram-positive bacterium. Titration data over a pH range of 3 to 11 were best fit with a three-site model, and the pK_a values were 5.2 $\pm$ 0.3, 7.5 $\pm$ 0.4, and 10.2 $\pm$ 0.5. Based on the average pK_a values for simple carboxylic (pK_a ~ 4-6), phosphoryl (~7-8), and phenolic hydroxide (~ 9-11), Daughney et al. (1998) assumed that the pK_a values corresponded to carboxyl, phosphoryl, and hydroxyl surface functional groups, respectively. Fein et al. (1997) found similar pK_a values for the surface-binding sites on *Bacillus subtilis* cell surfaces: 4.8 $\pm$ 0.2, 6.9 $\pm$ 0.5, and 9.4 $\pm$ 0.6. Unlike Gram-positive bacteria, structures and compositions of Gram-negative bacteria are different; the amino acid composition in the Gram-

negative bacteria is higher due to a mixture of lipopolysaccharides and protein in the outer membrane (Haas et al., 2001).

Surface-complexation models (SCMs) were used to predict the extent of metal and radionuclide sorption by bacteria in response to changes in environmental parameters such as pH, bacteria-to-metal ratio, ionic strength, and temperature (e.g., Fein et al., 1997; Daughney and Fein, 1998; Daughney et al., 1998; Xue et al., 1998; Fowle and Fein, 1999). Metals in solution can complex with surface-functional groups, much like they complex with the same groups in solution. For Np(V), the dominant species for pH $\leq$ 8 is NpO_2^+, which can complex with deprotonated surface sites. We show the complexation reaction and stability constant for NpO_2^+ with the carboxylic surface group as an example:

$$\equiv X - COO^- + NpO_2^+ \rightarrow \equiv X - COO(NpO_2)^0 \quad \textbf{(9)}$$

$$K_5 = \frac{[\equiv X - COO(NpO_2)^0]}{[\equiv X - COO^-]\{NpO_2^+\}} \quad \textbf{(10)}$$

At high pH, NpO_2^+ declines, and Np(V)-carbonate species begin to dominate. The Np(V)-carbonate complexes are likely to sorb onto the $\equiv X - NH_3^+$ surface sites are:

$$\equiv X - NH_3^+ + NpO_2CO_3^- \rightarrow \equiv X - NH_3(NpO_2CO_3) \quad \textbf{(11)}$$

$$\equiv X - NH_3^+ + NpO_2(CO_3)_2^{3-} \rightarrow \equiv X - NH_3(NpO_2(CO_3)_2)^{2-} \quad \textbf{(12)}$$

$$\equiv X - NH_3^+ + NpO_2(CO_3)_3^{5-} \rightarrow \equiv X - NH_3(NpO_2(CO_3)_3)^{4-} \quad \textbf{(13)}$$

The surface complexation of Np depends on the pH-dependent Np speciation and bacterial surface species. Thus, surface complexation of Np(V) should depend on pH in a complicated manner that involves the speciation of the surface sites and Np(V) in solution. Therefore, our goal was to characterize the Np(V)-complexation sites on surface components of *S. alga*.

2. MATERIALS AND METHODS

2.1. Growth of *Shewanella alga* strain *BrY*

Shewanella alga strain *BrY*, a dissimilatory metal-reducing and Gram-negative rod, was isolated from the Great Bay Estuary, New Hampshire (Caccavo et al., 1992). It is a facultative anaerobe that can grow rapidly under aerobic conditions. We grew it aerobically on tryptic soy broth 24 hours prior to use. Cells were harvested from stationary phase at an optical density at 600 nm (OD_{600}) of 0.1 and rinsed three times in a solution of 0.01 M PIPES (piperazine-N, N'-bis[2-ethanesulfonic acid]) and 0.1 M KCl. The pH of the rinse solution was the same as that used in the subsequent batch experiments. The rinsed cells were concentrated by centrifugation at 4400 rpm and 4°C, and then they were re-suspended to prepare an inoculum stock with a final OD_{600} between 1 and 2.

2.2. Cell-Wall Purification

To isolate the bacterial cell walls, we modified a method developed by Salton (1964), who used sonication for homogenization followed by differential centrifugation for fractionation. Cell-wall isolation began by disrupting the cells in 0.1 M KCl solution with sonication (B. Braun Labsonic® U sonicator, B. Braun Biotech International). The cell suspensions were sonicated 5 times for 1 min (rested 1 min in an ice bath between bursts) at the power of 100 W and the frequency of 20 kHz. The degree of disruption was monitored by phase microscopy. The disrupted cells were centrifuged at 20000 g (Optima TLX Ultracentrifuge 120000 rpm, Beckman Coulter, Inc.), and the pellets were resuspended in 0.1 M KCl and centrifuged at 5000 g for 5 min to remove intact cells and coarse debris. Then, the isolated cell walls were collected at

13000 g for 20 min.

2.3. EPS Isolation

We modified the method developed by Yildiz and Schoolnik (Yildiz and Schoolnik, 1999) to extract EPS from *S. alga*. First, *S. alga* was cultivated overnight at 30°C on the surface of sterile cellophane dialysis membranes (Sigma-Aldrich Co., St. Louis, MO) placed on the surface of tryptic soy broth agar plates. The lawn of confluent biomass growth was harvested and suspended in 250 ml of 0.9% NaCl. The EPS were then detached from the bacterial surface by centrifuging them at 13000 g for 1 hour at 4°C, which removed pellets of intact cells. Crude EPS were precipitated from the supernatant after adding 750 mL of 100% ethanol and refrigerating it overnight. The EPS precipitate was centrifuged at 13000 g for 30 min with 95% ethanol twice and with 100% ethanol once. Then, the pellets of EPS were collected and allowed to dry.

2.4. Titration Experiments

We performed acid or base titrations to determine the density and pK_a values of surface acid/base groups. Titration experiments were carried out using a potentiometric auto-titrator (Model KEM AT210, Kyoto Electronics Manufacturing Co., Ltd.) with a 20-mL burette unit (Model APB-118-01B). Solutions were degassed for 20 min with N_2 and kept in a N_2 anaerobic chamber (Plas Labs) when not in use to keep out O_2 and CO_2, which could affect the pH. The titrant solutions and titrant aliquot were degassed again immediately prior to titration and kept under positive pressure of N_2 by allowing a gentle flow of N_2 through the entire system during the titration.

We used a 'down-up pH' protocol for the titration experiment. A known amount of bacterial cells was added to a 0.1-M $NaNO_3$ solution. The solution was then divided into two portions, each of 30-ml volume. The first portion was added into the titration vessel and titrated with 0.1 M HNO_3 to a pH value of 4. Then, the titration vessel was cleaned of the first portion. The second portion was added and titrated with 0.1 M NaOH to a pH value of 10. The overall results were combined to produce the entire titration spectrum. The reason for using the 'down-up pH' method was to preclude alterations of the biomass by extreme pH.

At each titration point, the auto-titrator recorded a potential value of the bacterial cell suspension and the corresponding amount of acid or base added. The potentials were converted to the pH of the cell suspension. At each point, we allowed the sample to equilibrate at a new pH for at least 3 minutes or once a potential stability of 0.1 mV/s had been attained.

2.5. Effects of Extreme pH

To determine if pH extremes altered the biomass's acid/base characteristics, we adjusted the pH of whole-cell suspensions directly to 2 or 12 with concentrated HNO_3 or NaOH. The suspension at pH 2 was then titrated with 0.1 M NaOH, while the suspension at pH 12 were titrated with 0.1 M HNO_3 with the method described above.

2.6. Preparation and analysis of NpO_2^+

The isotopic purity of the neptunium used was greater than 99% by mass and 87% by curies based on isotopic analysis. All original Np was first oxidized to NpO_2^{2+} by fuming in perchloric acid and then reduced to pentavalent neptunyl, NpO_2^+, by the addition of a few drops of 30% hydrogen peroxide (based on Seaborg and Katz, (1954) and Clark et al. (1995)). The

pentavalent neptunyl was precipitated as a sodium-neptunium-carbonate phase, washed with high purity water, and dissolved in 0.1 M perchloric acid to form the stock solution. The oxidation state of this neptunium stock was established by absorption spectrometry (always >99% oxidation-state purity). This stock was added to the PIPES/KCl solution prior to starting the batch experiments. Neptunium(V) concentrations were determined by α-scintillation counting (Collins, (1960)) and periodically verified by inductively coupled plasma-mass spectroscopy (ICP-MS) (VG Model Elemental PQII$^+$ Turbo ICP/MS).

2.7. Batch Experiments of Np(V) Surface Complexation

We performed batch experiments to establish the rate and concentration dependence of neptunium complexation onto *S. alga* cell surfaces. Batch experiments were carried out in 1.5-mL centrifuge tubes containing 1 mL of 0.1 M $NaNO_3$ solution under non-growth conditions. A known amount of biomass solid (i.e., bacterial whole cells, cell wall, or EPS) was added to the medium. The pH of the solution was adjusted prior to the experiments by adding a small amount of 0.2-μm-filtered NaOH or HNO_3. Aliquots from a concentrated Np(V) stock solution were added to bring the initial neptunium concentration to approximately 6 μM. To establish the stability of NpO_2^+ in solution, controls with no biomass additions were prepared. Bottles were gently shaken at 25 ± 2°C throughout the sorption experiments.

For each experiment, aliquots of 0.5 mL were drawn from the centrifuge tubes and analyzed for neptunium concentration after 120 minutes, which was long enough to establish equilibrium (Haas et al., 2001; Gorman-Lewis et al., 2005). The total neptunium concentration and the neptunium concentration after filtration through a 0.22-μm filter (Millipore UFC30GV25) were determined by α scintillation counting (Packard model 2500 TR liquid

scintillation analyzer) of duplicate samples. The amount of biomass-associated neptunium was calculated as the difference between the total and filtered concentrations of neptunium.

2.8. FITEQL

FITEQL is a non-linear least-square fitting program used to determine optimum model parameter values from a set of titration data at a single ionic strength or at multiple ionic strengths (Herbelin and Westall, 1994). The program optimizes the values of adjustable parameters by changing their values until the sum of the squares of the residuals between the measured titration data and FITEQL calculated values is minimized.

Deprotonation of the cell-surface functional groups creates negatively charged surface sites that give a negative electrical potential. This potential can affect the interactions of ions with the bacterial surface sites. We accounted for the effects on surface acidity constants with the relationship $K = K_{int} \exp\left(\frac{-ZF\psi}{RT}\right)$. We related the electric potential (ψ) to the surface charge (σ) using a constant capacitance model for the electric field $C = \frac{\sigma}{\psi}$, where C is the capacitance of the bacterial surface in F/m^2 (Stumm and Morgan, 1996). We used a capacitance of 8 F/m^2, which is the same value used by Fein et al., 1997 for *B. subtilis*. FITEQL uses the Davies equation (Herbelin and Westall, 1994) to calculate ionic strength and activity coefficients for species in solution.

FITEQL calculates the variance, V(Y), between the experimental data and the model, which provides a quantitative means of comparing the fit of the different models.

$$V(Y) = \frac{\sum \left(\frac{Y_{calc} - Y_{exp}}{S_{exp}} \right)^2}{n_p n_{II} - n_u} \qquad (14)$$

where Y_{calc} and Y_{exp} are the calculated and the experimental data, S_{exp} is the error associated with the experimental data, n_p is the number of data points, n_{II} is the number of Group II components (total and free concentrations are known), n_u is the number of adjustable parameters, and V(Y) is the variance in Y. The V(Y) value provides a quantitative measure of the goodness of fit of each model, and we use this parameter to determine the best-fitting model. The rule of thumb is that reasonable fits correspond with V(Y) values of between 1 and 20 (Herbelin and Westall, 1994).

S. alga is rod shaped, with a length of 2.2 μm and a 0.63-μm diameter (Caccavo et al., 1996), yielding a geometric surface area of 4.98×10^{-12} m^2/cell. Based on plate counting, a bacterial suspension of 1 g cells/L is composed of 9.1×10^9 cells/mL. Coupling the geometry and mass factor for *S. alga* yields a specific surface area of 45 m^2/g.

2.9. CCBATCH Speciation Model

We used the SPECIATE subroutine in the biogeochemical model CCBATCH to calculate Np(V) speciation in solution (VanBriesen and Rittmann, 1999, 2000). Table 1 presents the parameter inputs we used for CCBATCH.

Table 1
Complex formation constants for major aqueous species used in CCBATCH (Smith et al., 1997).

Species	β_{xyz} [a]
NpO_2OH	$\beta_{1(-1)0} = 10^{-9.1}$
$NpO_2(OH)_2^-$	$\beta_{1(-2)0} = 10^{-23.1}$
$NpO_2CO_3^-$	$\beta_{101} = 10^{4.1}$
$NpO_2(CO_3)_2^{3-}$	$\beta_{102} = 10^{7.1}$
$NpO_2(CO_3)_3^{5-}$	$\beta_{103} = 10^{8.5}$
NpO_2Cl	$\beta_{101} = 10^{-0.35}$
NpO_2NO_3	$\beta_{101} = 10^{-0.6}$
HCO_3^-	$\beta_{011} = 10^{9.9}$
H_2CO_3	$\beta_{021} = 10^{6.1}$
$NaOH$	$\beta_{1(-1)0} = 10^{-13.9}$
$NaCO_3^-$	$\beta_{101} = 10^{1.3}$
$NaHCO_3$	$\beta_{111} = 10^{-0.25}$
HCl	$\beta_{011} = 10^{-3}$
$NaCl$	$\beta_{101} = 10^{-0.5}$
HNO_3	$\beta_{011} = 10^{-0.78}$
$NaNO_3$	$\beta_{101} = 10^{-0.55}$

(a) Where $\beta_{xyz} = \dfrac{[M_x H_y L_z]}{[M]^x [H]^y [L]^z}$ or $\beta_{x(-y)z} = \dfrac{[M_x (OH)_y L_z][H]^y}{[M]^x [L]^z}$

3. RESULTS AND DISCUSSION

3.1. Effects of Extreme pH on *S. alga*

Exposure of *S. alga* whole cells to extreme pH caused three effects. First, exposure to pH 2 caused the cells to aggregate, which was visibly observable. Second, titration with NaOH of cells exposed to pH 2 resulted in a loss of buffering capacity, probably because of loss of surface functional groups, perhaps from denaturation of the cell proteins or loss of exposed surface site due to aggregation. Third, exposure to pH 12 resulted in a loss of optical density, most likely due to hydrolysis of cell solids (Madigan et al., 2000).

The extreme-pH results demonstrate why we used the 'down-up pH' protocol (i.e., starting from around neutral pH, one portion of identical aliquots was titrating up-pH with NaOH and the other titrating down-pH with HNO_3) and stopped pH titrations at 4 and 10. We kept these pH limits to preserve the chemical properties of the cell components, which were destroyed when the starting pH was in the extreme pH regions.

3.2. Calculating the Deprotonation Constants of Surface Functional Groups on *S. alga* Whole Cells, Cell Walls, or EPS using FITEQL

We used FITEQL version 4.0 (Herbelin and Westall, 1994) to solve for the deprotonation constants and absolute concentrations (mole/L) of each distinct type of surface sites. For each titration, we fit the titration experimental data by employing models involving one, two, or three distinct types of surface functional groups. FITEQL was unstable when we tried to use four groups, and this prevented us from testing a four-site model. We normalized the surface site

concentrations (mole/L) to the weight of biomass per liter of electrolyte, yielding specific site concentrations in moles per gram of bacterial cells or cell component suspensions.

Figure 1 compares the best-fit modeling results with the experimental results from the titration experiment with 10.1 gram of *S. alga* whole-cell dry weight/L. The experimental data were fit well only by a model having three distinct types of surface functional groups. Models including only one or two distinct types of surface functional groups did not adequately fit all of the experimental data. A one-site model with a pK_{a1} of 10.2 could account for the buffering capacity of the bacterial suspensions only above pH 8. The one-site model failed totally for pH less than 8. Similarly, the two-site model with pK_as of 9.5 and 6.7 described the experimental data above pH 6, but had almost no buffering capacity for pH less than 5. The V(Y) values also were well out of the acceptable range for one and two groups.

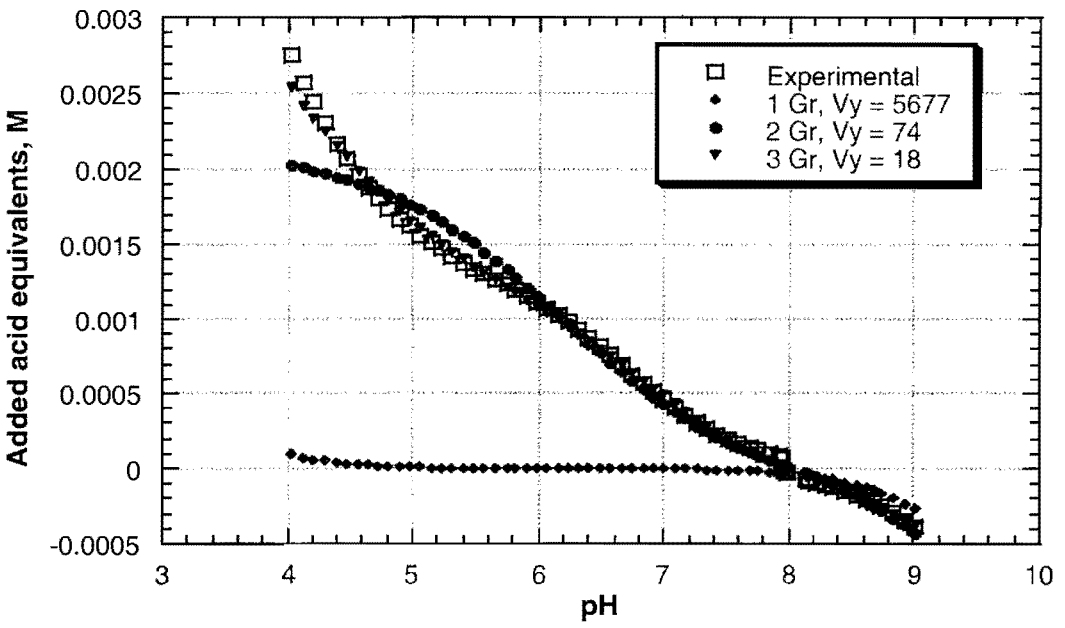

Fig. 1. Comparison of the experimental data with one-, two-, and three-site modeling results from FITEQL for 10.09 g of *S. alga*/L. The capacitance was 8 F/m^2. The pK_a values for each set of functional groups are: 3 groups, pK_as = 5.0, 7.2, and 10.0; 2 groups, pK_as = 6.7 and 9.5; and 1 group, pK_a = 10.2.

The three-site model showed the proper buffering capacity for the entire pH range with best-fit pK_a values of 5.1 $\pm$ 0.4, 7.2 $\pm$ 0.3, and 10.0 $\pm$ 0.3. Although direct analysis of the bacterial cell surfaces is required for confirming the existence of these surface functional groups, we interpret that the three pK_a values of 5.1, 7.2, and 10.0 correspond to carboxyl, phosphoryl, and amino groups, respectively, which are commonly present on Gram-negative cell surfaces (Haas et al., 2001). The corresponding concentrations for the three functional groups on *S. alga* were 3.1×10^{-3} moles, 1.4×10^{-3} moles, and 4.3×10^{-3} moles of the surface sites per gram of bacteria.

We also used FITEQL to solve for the deprotonation constants and the concentrations of each functional group on *S. alga* cell walls and EPS. As Fig. 2 shows, the titration data for *S. alga* cell walls and EPS also were fit well by a model having three distinct types of surface functional groups. Table 2 lists all the pK_a values and specific site concentrations for isolated cell walls and EPS, as well as for whole cells. The pK_a values were similar for whole cells, purified cell walls, and EPS: 4.8 to 5.2 for pK_{a1}, 7.2 to 7.3 for pK_{a2}, and 10.0 to 10.9 for pK_{a3}.

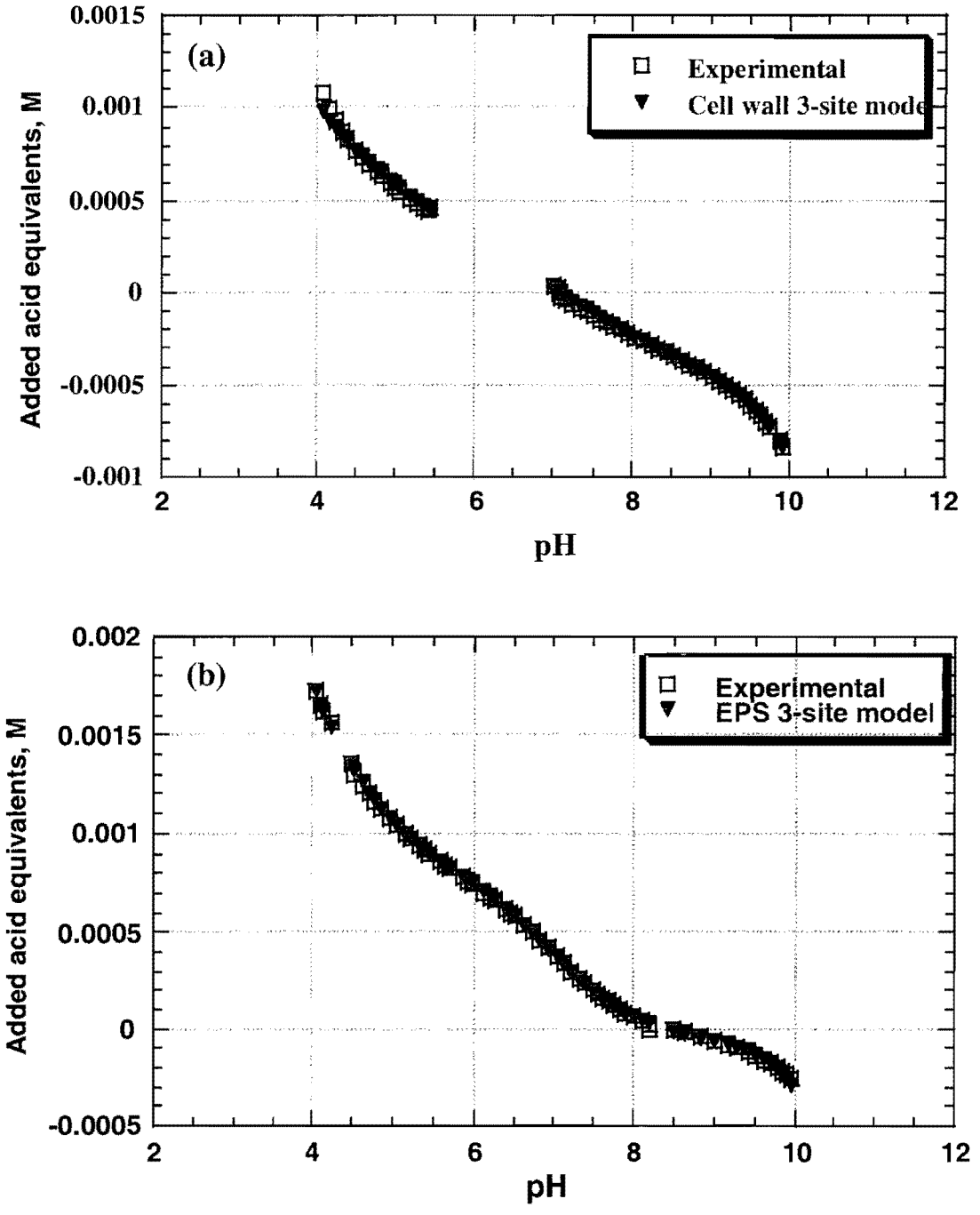

Fig. 2. Comparison of the experimental data with the three-site modeling results from FITEQL for (a) 0.77 g of cell wall/L and (b) 9.75 g of EPS/L. The capacitance was 8 F/m^2. The pK_a values for cell wall modeling run are 5.2, 7.2, and 10.2. The pK_a values for EPS modeling run are 4.8, 7.3, and 10.9.

Table 2
The pK_a values and specific site concentrations for the best-fit three-site models for *S. alga* cell walls, EPS, and whole cells.

Cell Component	pK_{a1}[a]	C_{S1}[b]	pK_{a2}	C_{S2}	pK_{a3}	C_{S3}	**ΣCs**	**V(Y)**
Cell Walls	5.16	6.8 (46.4%)	7.2	0.74 (5.1%)	10.2	7.1 (48.5%)	14.6	9.7
EPS	4.76	2.2 (35.2%)	7.28	0.88 (14.5%)	10.9	3.0 (49.3%)	6.1	7.8
Whole Cells	5.1	3.1 (35.2%)	7.2	1.4 (15.9%)	10.0	4.3 (48.9%)	8.8	18

(a) pK_a values for the surface functional groups correspond to the condition of zero ionic strength and zero charge coverage.
(b) Absolute concentrations of the surface functional groups are in mmoles per gram of bacterial cell component. Percentages of the row totals are in parentheses.

Approximately 20 commonly occurring amino acids polymerize to form peptides and proteins. Amino and carboxyl groups on amino acids react in a head-to-tail fashion, eliminating a water molecule and forming a peptide bond as a backbone structure of proteins. Voet and Voet (1995) listed the pK_a of the terminal amino groups on amino acids ranging from 8.8 to 11.0, while terminal carboxylate groups have pK_a values near 2.4. Several amino acids -- aspartic acid, glutamic acid, histidine, arginine, lysine, and serine -- contain a side chain group that has acid/base properties. For example, aspartic acid and glutamic acid contain a side chain with a carboxyl functional group; histidine, arginine, and lysine contain a side chain with an amino functional group; and serine contains a side chain with a hydroxyl functional group. The pK_a values of R groups of aspartic acid, glutamic acid, histidine, arginine, lysine, and serine are 3.9, 4.3, 6.0, 12.5, 10.5, and 13, respectively. Thus, proteins possess reactive amino and carboxyl termini, and they further display characteristics of the side chain groups that have acid/base properties with a range of pK_a values.

Based on the typical pKa values of the common functional groups discussed above, the functional groups with the pK_a value of 4.8 to 5.2 most likely correspond to the carboxyl functional groups from polysaccharides or from side chains of amino acids and proteins, the functional groups with the pK_a value of 7.2 to 7.3 most likely correspond to the phosphoryl functional groups from phospholipids, and the functional groups with the pK_a value of 10.0 to 10.9 most likely correspond to the terminal amino groups or the side chain of amino acids from proteins.

The amino groups (C_{s3}), comprising about 50% of the total sites (Table 1), were the most plentiful in bacterial whole cells, cell walls, and EPS. The second largest group, from 35% to 46%, was carboxyl (C_{s1}) for all three components.

Bacterial cell walls displayed the highest total site density (ΣC_s), and the cell-wall sites were dominated by the carboxyl and amino groups, with few phosphoryl groups. Cell walls are composed mainly of polysaccharides and peptidoglycans, macromolecules that contain carboxyl and amino functional groups. Having the least phosphoryl groups indicates that cell walls have the least phospholipids, which house the phosphoryl sites. Phosphoryl groups were greatest in the whole cells, but always the group having the fewest functional groups. Based on the distribution of the three sites and the total site density, the whole cells have acid/base properties more similar to EPS than to cell wall.

3.3. Determining Site-Specific Stability Constants for Np(V) Adsorption onto *S. alga* Cell Surfaces

After obtaining the concentrations and the deprotonation constants for the surface site reactions, we used CCBATCH to determine site-specific stability constants for Np(V) adsorption

onto bacterial surfaces from batch metal-sorption experiments containing fixed biomass concentrations, a fixed initial Np(V) concentration, and 0.1 M $NaNO_3$. Figure 3 shows the amount of Np(V) adsorbed over the pH range for whole cells, cell wall, and EPS. It also presents the best-fit modeling results, which are described below.

Figure 4 shows the corresponding Np(V) aqueous-phase speciation, as computed by the speciation sub-model of CCBATCH. At pH less than 4, almost all Np(V) is NpO_2^+ ion. A carboxyl group with pK_a of 5.0 is nearly absent at a pH of 4 or lower. This means that Np complexes with the surface functional groups should have been negligible for pH less than 4. However, the experimental data (Fig. 3) clearly show that Np(V) complexed to the bacterial surface sites for this low-pH range. The likely explanation for this continued Np(V) complexation at low pH is that another surface functional group existed and had a lower pK_a. We propose that this group is X-COOH from amino acids, which typically have pK_a values near 2.4 (Voet and Voet, 1995). The presence of an amino acid X-COOH group could not be detected by the pH titration, because the titrations must proceed to a pH well below 2 to fully define a pK_a of 2.4. However, because the biomass aggregated and lost acid/base functional groups at pH approaching 2, we could not quantify the amino X-COOH group, even though it existed. However, the surface-complexation effect of amino $X\text{-}COO^-$ groups can be detected at pHs well above $pK_a \sim 2.4$, as is illustrated in Fig. 3.

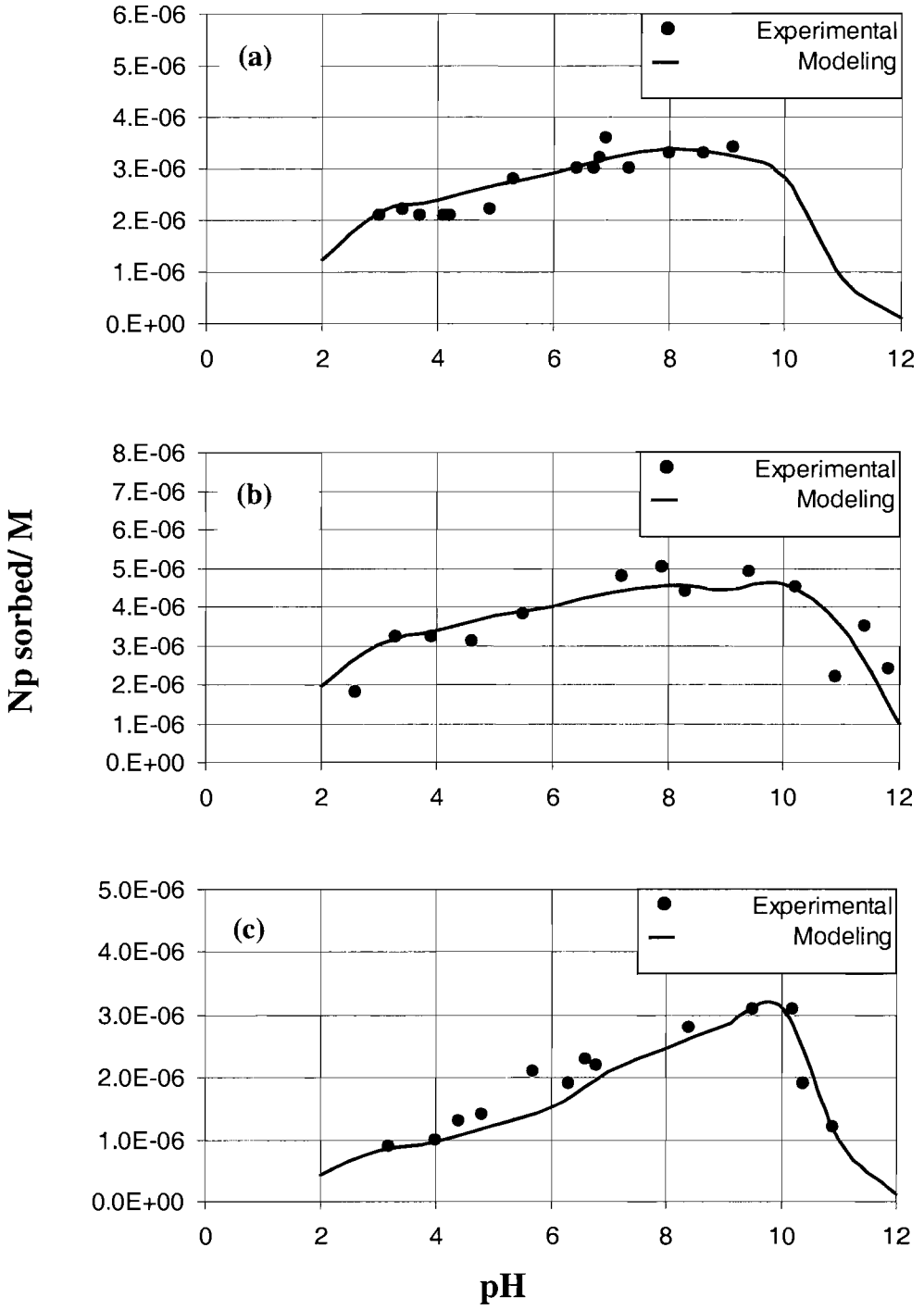

Fig. 3. Comparison of experimental and modeling results for Np(V) surface complexation by *S. alga* components as a function of pH and suspended bacterial concentrations for (a) whole cell – 3.7 g/L, (b) EPS – 9.75 g/L, and (c) cell wall – 0.77 g/L.

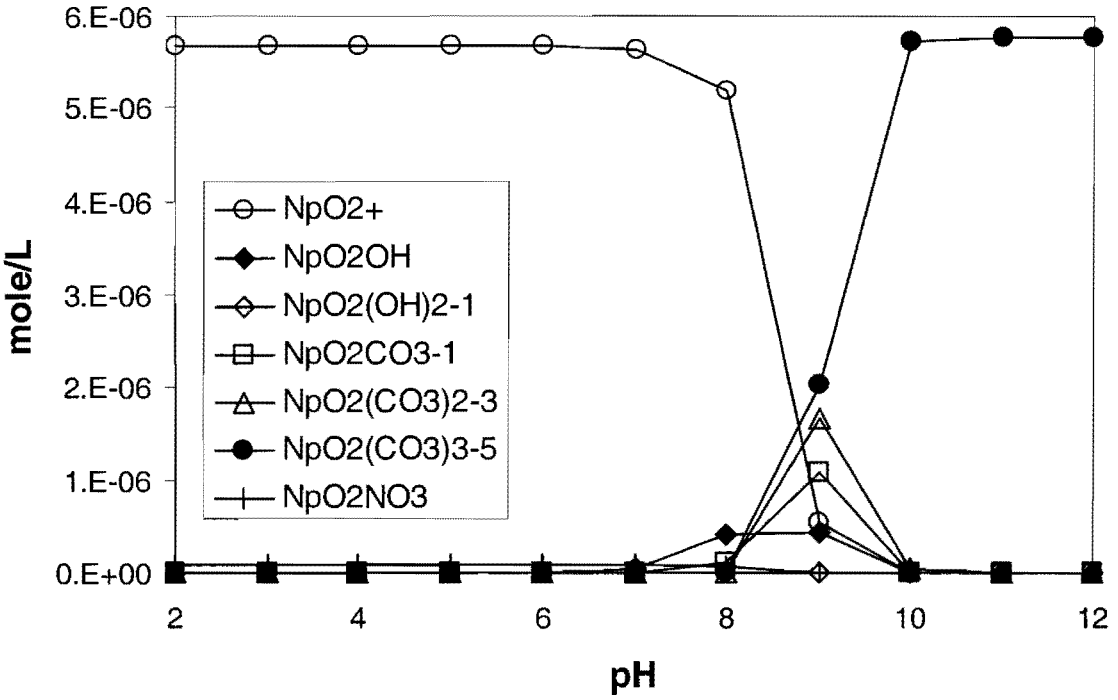

Fig. 4. Np(V) speciation as a function of pH in 0.1 M $NaNO_3$ electrolyte, in equilibrium with carbonate in the atmosphere, and with 5.76 μM initial Np(V) concentration.

3.4. Proposing an Additional Carboxyl Surface Site with pK_a of 2.4

Although we cannot detect the low-pK_a carboxyl groups associated with amino acids from the titration experiment, we were able to see them with Np(V) complexation experiments that did not go below pH 3. Therefore, we propose that an additional carboxyl surface site with pK_a of 2.4 existed, based on the fact that amino-acid groups were present. Since the low-pK_a carboxyl groups come from the same amino acids, we further propose that the concentration of the low-pK_a carboxyl groups was equal to the concentration of the amino groups obtained from FITEQL calculations. The concentration is thus 4.3×10^{-3} moles per gram of *S. alga* whole cells, 5.7×10^{-3} moles per gram of cell wall, and 3.0×10^{-3} moles per gram of EPS. Adding the low pK_a group did not alter the best-fit titration curves in Figures 1 and 2 (not shown).

We coupled the experimental data (Fig. 3) with CCBATCH-computed speciation and surface-site speciation to explain the features of the pH-dependent Np(V) surface complexation and to generate the model results also shown in Fig. 3. We show in detail how we extracted the log K values for *S. alga* whole cells. Later, we list the calculated Np(V) surface-complexation stability constants for isolated cell wall and EPS, obtained with the same procedures.

We determined the absolute concentrations of each functional group in mole/L for CCBATCH input parameters by multiplying the known biomass or cell component concentration in gram/L for each experiment by the concentration in mol/g of bacteria.

Figure 5 illustrates the new pH-dependent surface site speciation for whole cells with 4 functional groups, i.e., low-pK_a carboxyl (pK_a of 2.4), carboxyl (pK_a of 5.1), phosphoryl (pK_a of 7.2), and amino (pK_a of 10.0) groups. Figure 4 shows the corresponding pH-dependent speciation for Np(V).

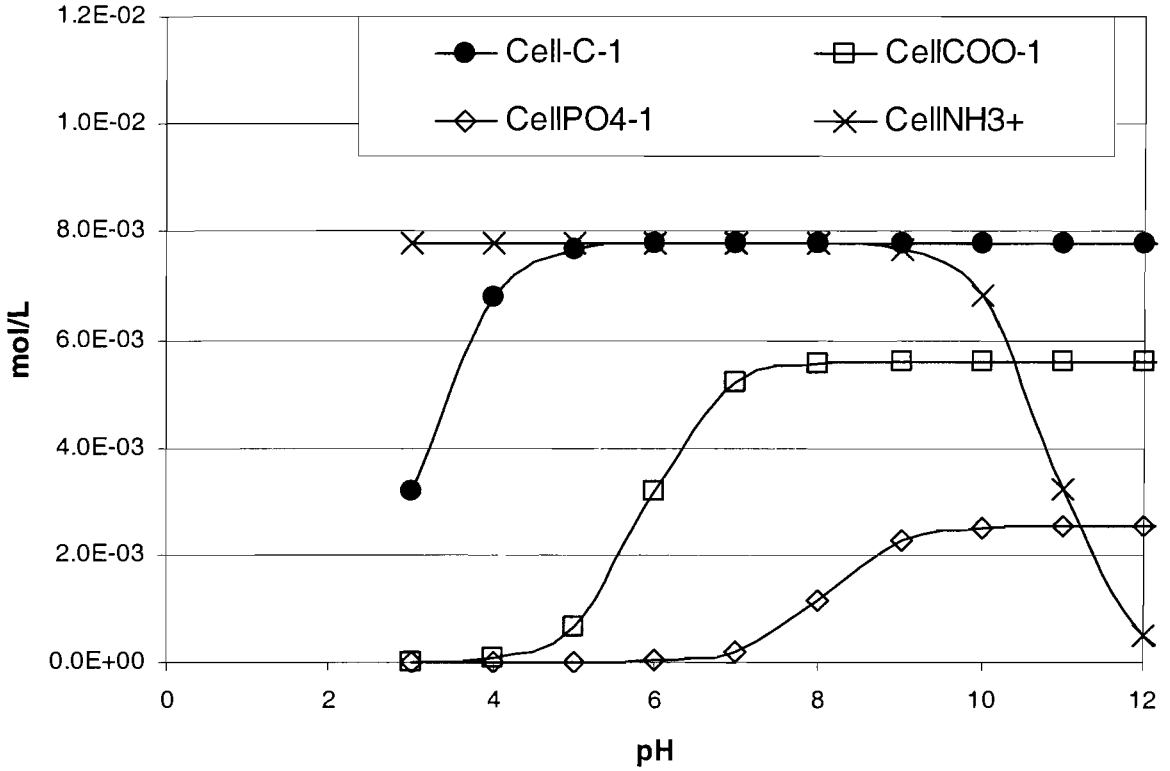

Fig. 5. Bacterial surface sites as a function of pH, with FITEQL-calculated 4 pK_a values of 2.4, 5.1, 7.2, and 10.0 and with the concentrations of $7.78x10^{-3}$ moles/L of low-pK_a carboxyl groups, $5.61x10^{-3}$ moles/L of carboxyl groups, $2.53x10^{-3}$ of phosphoryl groups, and $7.78x10^{-3}$ moles/L of amino groups. The $>XC^-$ represents the low-pK_a carboxylate groups. (From CCBATCH)

3.5. Determining the Stability Constants for $>XCNpO_2$ and $>XCOONpO_2$ from the pH Range of 2 to 4

In this pH range, the dominant Np(V) species is the NpO_2^+ free ion (Fig. 4), and the dominant ligand surface species is $>XC^-$, the low-pK_a carboxyl groups, although $>XCOO^-$ begins to become significant for pH near 4 (Fig. 5)

We used the speciation model in CCBATCH to calculate the best-fit stability constants for NpO_2^+ complexation with $>XC^-$ and $>XCOO^-$. In a CCBATCH input file, we specified each surface site and NpO_2^+ as **components**. The metal, i.e., NpO_2^+, complexed onto each bacterial surface site was specified as a **complex** or **species**. The components were H^+, NpO_2^+, H_2CO_3, X^-

C^-, and X-COO^-. The species for the system were OH^-, CO_3^{2-}, HCO_3^-, X-CH, X-COOH, NpO_2OH, $NpO_2CO_3^-$, $NpO_2(CO_3)_2^{3-}$, $NpO_2(CO_3)_3^{5-}$, X-$CNpO_2$, and X-$COONpO_2$. In this pH range, the complexation of NpO_2^+ onto bacterial surface functional groups can be described by

$$\equiv X - C^- + NpO_2^+ \rightarrow \equiv X - C(NpO_2)^0$$

and $$\equiv X - COO^- + NpO_2^+ \rightarrow \equiv X - COO(NpO_2)^0$$

In the CCBATCH calculation, the log K values of X-$COONpO_2$ and X-$CNpO_2$ species are adjustable parameters. We adjusted the (log K)s to minimize the difference between the input experimental value for adsorbed Np(V) (i.e., total sorbed Np(V) as a function of pH) and the calculated value for sorbed Np(V) (i.e., the sum of the X-$COONpO_2$ and X-$CNpO_2$ concentrations). The best-fit log K stability constants for Np(V) adsorption for the low-pK_a carboxyl and the other carboxyl group were 1.75 and 1.75. The calculated log K values are in good agreement with the log K values for Np(V) complexation with other carboxylate-containing ligands, such as acetate (1.46), lactate (1.56) and succinate (1.72) (Smith et al., 1997).

3.6. Determining the Stability Constants for >XPO_4NpO_2 from pH Range of 4 to 8

In this pH range, the dominant Np(V) aqueous species still was the NpO_2^+ free ions (Fig. 4), and the significant ligand surface species were >XC^-, >$XCOO^-$, and >XPO_4^-, with >$XCOO^-$ rising sharply throughout the range (Fig. 5). Using the log K values for the two carboxyl groups obtained from the previous step, we further used CCBATCH to determine the stability constant for >XPO_4NpO_2 that best-fit the experimental data in the pH range 4 to 8. The sorption of NpO_2^+ onto phosphoryl functional groups can be described by

$$\equiv X - PO_4^- + NpO_2^+ \rightarrow \equiv X - PO_4(NpO_2)^0$$

The additional component for CCBATCH input file was >X-PO_4^-, and the additional species were >X-PO_4H, and >X-PO_4NpO_2.

The best-fit log K value for Np surface complexation for the phosphoryl group was 2.20. The calculated log K values are in good agreement with the log K values for Np complexation with inorganic phosphate (2.54 for $NpO_2HPO_4^-$) (Smith et al., 1997).

3.7. Determining the Stability Constants for >X$NH_3NpO_2(CO_3)$ and >X$NH_3NpO_2(CO_3)_2^{2-}$ from the pH Range of 8 to 10

In this pH range, the dominant Np species shifted dramatically from NpO_2^+ to $NpO_2(CO_3)^-$, $NpO_2(CO_3)_2^{3-}$, and $NpO_2(CO_3)_3^{5-}$ species, with $NpO_2(CO_3)_3^{5-}$ becoming completely dominant by pH = 10 (Fig. 4). With the shift away from NpO_2^+ as the dominant Np(V) species, the important ligand surface group became >XNH_3^+. Sorption onto the amino functional groups can be described by

$$\equiv X - NH_3^+ + NpO_2CO_3^- \rightarrow \equiv X - NH_3(NpO_2CO_3)$$

$$\equiv X - NH_3^+ + NpO_2(CO_3)_2^{3-} \rightarrow \equiv X - NH_3(NpO_2(CO_3)_2)^{2-}$$

$$\equiv X - NH_3^+ + NpO_2(CO_3)_3^{5-} \rightarrow \equiv X - NH_3(NpO_2(CO_3)_3)^{4-}$$

The new component for CCBATCH input file was >X-NH_2, and the additional species were >X-NH_3^+, >X-$NH_3(NpO_2CO_3)$, >X-$NH_3(NpO_2(CO_3)_2)^-$, and >X-$NH_3(NpO_2(CO_3)_3)^{4-}$.

We calculated the best-fit log K values for >X$NH_3NpO_2(CO_3)_3^{4-}$, >X$NH_3NpO_2(CO_3)_2^{2-}$, and >X$NH_3NpO_2(CO_3)$ for the experimental data in the pH range of 8 – 10. The best-fit log K values were 3.1, 2.7, and 1.8, respectively. Clearly, >X$NH_3NpO_2(CO_3)_3^{4-}$ was the important surface complex in that its log K value was higher than for other surface ligands that complex with NpO_2^+. The complexation at high pH of the Np-carbonate species was observed as long as

the $>XNH_3^+$ surface ligand was present. The calculated log K values are in good agreement with the log K values for Np(V) complexation with N-containing carboxylates (3.4 for alanine and 3.6 for glycine (Smith et al., 1997).

Table 3 summarizes the C_s, pK_a, and log K values for Np(V) complexation to sites on whole cells of *S. alga,* as well as on the purified cell walls and isolated EPS. The best-fit stability constants for Np adsorption, along with C_s and pK_a values, also are given for the cell components in Table 3.

The comparisons between the modeling results and the experimental results in Fig. 3 show that the model captured the trends in Np(V) complexation to whole cells, cell walls, and EPS over the pH range of 2 – 12. For all biomass materials, Np(V) surface complexation increased nearly linearly from pH 4 to 8 due to $>XCOO^-$ and $>XPO_4^-$ ligands increasing as pH increases (Fig. 5). For pH 8 to 10, Np(V) sorption reached a plateau for whole cells and EPS due to the decline in NpO_2^+, which is compensated by the increases in $NpO_2(CO_3)^-$, $NpO_2(CO_3)_2^{3-}$, and $NpO_2(CO_3)_3^{5-}$, which complexes with the $>XNH_3^+$ surface ligand. Cell walls do not show the plateau, because they have much less of the phosphoryl surface groups to complex with NpO_2^+. The strong drop off of Np(V) sorption for pH > 10 with whole cells, EPS and cell walls was due to the decrease in $>XNH_3^+$ surface ligand.

Table 3
The log K values for Np adsorption onto functional groups on *S. alga* whole cells, cell walls, and EPS.

		Whole Cells			EPS			Cell Walls		
Functional Group	**Np-Complexed Species**	**pK_a[a]**	**C_S[b]**	**Log K**	**pK_a**	**C_S**	**Log K**	**pK_a**	**C_S**	**Log K**
>XCH	NpO_2^+	2.4	$4.3x10^{-3}$	1.75	2.4	$3.0x10^{-3}$	1.75	2.4	$7.1x10^{-3}$	1.75
>XCOOH	NpO_2^+	5.1	$3.1x10^{-3}$	1.75	4.8	$2.2x10^{-3}$	1.75	5.2	$6.8x10^{-3}$	1.75
$>XPO_4H$	NpO_2^+	7.2	$1.4x10^{-3}$	2.2	7.3	$8.8x10^{-4}$	2.5	7.2	$7.4x10^{-4}$	3.1
$>XNH_3^+$	$NpO_2(CO_3)^-$	10.0	$4.3x10^{-3}$	1.8	10.9	$3.0x10^{-3}$	2.0	10.2	$7.1x10^{-3}$	2.0
	$NpO_2(CO_3)_2^{3-}$			2.7			3.0			2.9
	$NpO_2(CO_3)_3^{5-}$			3.1			3.2			3.6

(a) pK_a values for the surface functional groups, corresponding to the condition of zero ionic strength and zero charge coverage.
(b) Absolute concentrations of the surface functional groups in moles per gram of bacterial cell component.

To summarize, solution pH influenced the metal speciation and the metal-binding sites on the bacteria cell surfaces. Using acid/base titrations and Np(V) sorption experiments, we characterized surface sites on three *S. alga* surface components. The bacterial whole cells, purified cell walls, and isolated EPS each display four functional groups having pK_a values of 2.4, 4.8 to 5.2, 7.2 to 7.3, and 10.0 to 10.9. We interpret that these pK_a values correspond to the carboxyl group on amino acids, other carboxyl groups, phosphoryl groups, and amino groups on amino acids. Each surface functional group displayed similar affinity for Np(V) complexation. The log K for NpO_2^+ complexed onto the low-pK_a carboxyl, other carboxyl, and phosphoryl groups were 1.75, 1.75, and 2.2 to 3.1, respectively. The log K for $NpO_2(CO_3)^-$, $NpO_2(CO_3)_2^{3-}$ and $NpO_2(CO_3)_3^{5-}$ complexed onto the amino groups was 1.8 to 2.0, 2.7 to 3.0 and 3.1 to 3.6, respectively.

The most predominant species of Np(V) was NpO_2^+ at pH below 8. At low pH (i.e., less than 4), NpO_2^+ was complexed to the carboxyl groups with pK_a of 2.4 forming the surface-complexed $>XCNpO_2$. As pH increased, NpO_2^+ also complexed with another carboxyl groups (pK_a of ~5.0), forming the surface-complex $>XCOONpO_2$. Then, NpO_2^+ complexed to the phosphoryl groups (pK_a of 7.2), forming the surface-complex $>XPO_4NpO_2$. When pH increased above 8, the NpO_2^+ species decreased, but the aqueous Np(V)-carbonate species became the predominant species. The Np(V) carbonate species complexed to the amino group on the cell surfaces, balancing out the decrease in NpO_2^+ surface-complexes. At pH above 10, however, Np(V) sorption decreased due to the decrease in the $>XNH_3^+$ surface sites.

The surface-complexation by whole cells was between that of EPS and the cell wall, but more similar to EPS. This similarity stemmed mainly from EPS and whole cells having less of the high-pK_a carboxyl groups and more phosphoryl groups than did the cell walls.

Our results indicate that the surface-complexation model can be used to quantify surface complexation of Np(V) onto *S. alga* bacterial whole cells, EPS, and isolated cell walls. The complex pictures of Np(V) adsorption to whole cells, EPS, and purified cell walls can be explained by the pH-dependent shifts in Np(V) speciation (from NpO_2^+ to $NpO_2(CO_3)_3^{5-}$ as pH increases) and the change in available surface ligand groups. Complexation of Np(V) to surface ligands is of similar strength to complexation to the same ligands in solution and not large.

ACKNOWLEDGEMENTS

The authors are grateful to Argonne National Laboratory for laboratory facilities. The research was supported, in part, by the Nuclear Energy Research Initiative (NERI), the Environmental Remediation Sciences Program (ERSP) of the United States Department of Energy, and the National Center for Genetic Engineering and Biotechnology, Thailand, for partial financial support.

REFERENCES

Banaszak J. E., Rittmann B. E., and Reed D. T. (1999) Subsurface interactions of actinide species and microorganisms: Implications for the bioremediation of actinide-organic mixtures. *J. Radioanal. Nuc. Ch.* **241**, 385-435.

Beveridge T. J. (1989) Role of cellular design in bacterial metal accumulation and mineralization. *Ann. Rev. Microbiol.* **43**, 147-171.

Beveridge T. J., Forsberg C. W. and Doyle R. J. (1982) Major sites of metal-binding in *Bacillus-licheniformis* walls. *J. Bacteriol.* **150**, 1438-1448.

Caccavo Jr. F., Blakemore R. P. and Lovley D. R. (1992) A Hydrogen-Oxidizing, Fe(III)-Reducing Microorganism from the Great Bay Estuary, New Hampshire. *Appl. Environ. Microbiol.* **58**, 3211-3216.

Caccavo Jr. F., Ramsing N. B. and Costerton, J. W. (1996) Morphological and metabolic responses to starvation by the dissimilatory metal-reducing bacterium *Shewanella alga BrY. Appl. Environ. Microbiol.* **62**, 4678-4682.

Clark D. L., Hobart D. E. and Neu M. P. (1995) Actinide carbonate complexes and their importance in actinide environmental chemistry. *Chem. Rev.* **95**, 25-48.

Collins J. C. (Ed.) (1960) In *Radioactive Wastes: Their Treatment and Disposal.* John Wiley & Sons, New York, NY.

Daughney C. J. and Fein J. B. (1998) The effect of ionic strength on the adsorption of H^+, Cd^{2+}, Pb^{2+}, and Cu^{2+} by *Bacillus subtilis* and *Bacillus licheniformis*: A surface complexation model. *J. Coll. Int. Sci.* **198**, 53-77.

Daughney C. J., Fein J. B. and Yee N. (1998) A comparison of the thermodynamics of metal adsorption onto two common bacteria. *Chem. Geol.* **144**, 161-176.

Fein J. B., Daughney C. J., Yee N. and Davis J. (1997) A chemical equilibrium model for metal adsorption onto bacterial surfaces. *Geochim. Cosmochim. Acta.* **61**, 3319-3328.

Fowle D. A. and Fein J. B. (1999) Competitive adsorption of metal cations onto two gram positive bacteria: testing the chemical equilibrium model. *Geochim. Cosmochim. Acta.* **63**, 3059-3067.

Gorman-Lewis D., Fein J. B., Soderholm L., Jensen M. P. and Chang M. -H. (2005) Experimental study of neptunyl adsorption onto Bacillus subtilis. *Geochim. et Cosmochim. Acta.* **69**, 4837-4844.

Haas J. R., Dichristina T. J. and Wade Jr. R. (2001) Thermodynamics of U(VI) sorption onto *Shewanella putrefaciens*. *Chem. Geol.* **180**, 33-54.

Herbelin A. L. and Westall J. C. (1994) *FITEQL.* A computer program for determination of chemical equilibrium constants from experimental data. Report 94-01. Version 3.1. Department of Chemistry, Oregon State University, Corvallis, OR.

Madigan M. T., Martinko J. M. and Parker, J. (2000) *Brock Biology of Microorganisms.* 9th Ed. Prentice Hall, Upper Saddle River, NJ.

Murray R. L. (1989) In *Understanding Nuclear Wastes.* 3rd Edition. Powell, J.A. (Ed.) Battelle Press, Columbus, OH.

Pearl M. (2000) Technologies for remediating radioactively contaminated land. *Nuc. Energy* **39**, 107-112.

Salton M. R. J. (1964) In *The Bacterial Cell Wall.* Elsevier Publishing Company, Amsterdam.

Seaborg G. T. and Katz J. J. (1954) In *The Actinide Elements.* McGraw-Hill, New York, NY.

Smith R. M., Martell A. E. and Motekaitis R. J. (1997) *NIST Critically Selected Stability Constants of Metal Complexes Database, Version 4.0.* NIST: Standard Reference Data Program. Gaithersburg, MD.

Stumm W. and Morgan J. J. (1996) In *Aquatic Chemistry.* 3rd Ed. John Wiley and Sons, New York, NY.

VanBriesen J. M. and Rittmann B. E. (1999) Modeling speciation effects on biodegradation in mixed metal/chelate systems. *Biodegrad.* **10**, 315-330.

VanBriesen J. M. and Rittmann B. E. (2000) Mathematical description of microbiological reactions involving intermediates. *Biotechnol. Bioeng.* **68**, 705-705.

Voet D. and Voet J. G. (1995) In *Biochemistry.* John Wiley and Son, New York.

Xue H. B., Stumm W. and Sigg, L. (1988) The binding of heavy metals to algal surfaces. *Water Res.* **22**, 917-926.

Yildiz F. H. and Schoolnik G. K. (1999) *Vibrio cholerae* O1 El Tor: Identification of a gene cluster required for the rugose colony type, exopolysaccharide production, chlorine resistance, and biofilm formation. *Proc. Nat. Acad. Sci. U.S.A.* **96**, 4028-4033.